Evidence for a transition from weak to strong ferromagnetism from spontaneous resistivity anisotropy and high-field magnetic susceptibility data in amorphous $(Fe\text{-}Ni)_{80}$ $(P\text{-}B)_{20}$ alloys

S. N. Kaul and M. Rosenberg
Institut für Experimentalphysik VI, Ruhr-Universität Bochum, D-4630 Bochum 1, West Germany
(Received 22 November 1982)

The magnetoresistivity (both longitudinal and transverse) and high-field magnetic susceptibility χ_{hf} measurements have been performed on the glassy alloy series $Fe_xNi_{80-x}B_{20}$ and $Fe_xNi_{80-x}P_{14}B_6$ ($10<x<80$ at. %) at 4.2 K in fields up to 7 and 15 kOe, respectively. While the split-band model fails to account for the present results, the observed composition dependence of the spontaneous resistivity anisotropy (SRA) finds a straightforward explanation in terms of the two-current conduction model. Based on this model, the composition dependence of spin-up $\rho_\uparrow^0$ and spin-down $\rho_\downarrow^0$ residual resistivities has been computed. The computed variation of $\rho_\uparrow^0$ and $\rho_\downarrow^0$ with composition is shown to provide conclusive evidence not only for a transition from weak to strong ferromagnetism at a concentration $x\simeq 60$ at. % in the amorphous $Fe_xNi_{80-x}P_{14}B_6$ alloy series, but also for weak ferromagnetism in $Fe_xNi_{80-x}B_{20}$ glasses in the entire composition range. The difference in the ferromagnetic behavior of the two amorphous alloy series studied here has been explained by taking into account the charge transfer from the metalloid atoms to the transition-metal d bands. These observations are further supported by the χ_{hf} data. Furthermore, it is shown that no direct correlation exists between SRA and the saturation magnetization.

I. INTRODUCTION

Considerable interest devoted recently to the study of galvanomagnetic properties of amorphous transition-metal—metalloid (TM-M) alloys stems from the fact that such studies give a lot of useful information about the electronic structure of these alloys. One of the most informative tools among these properties is the spontaneous resistivity anisotropy (SRA) defined by $\Delta\rho_s/\rho_0=(\rho_{\|s}-\rho_{\perp s})/\rho_0$, where ρ_0 is the electrical resistivity in zero internal magnetic field (H_{int}), and $\rho_{\|s}$ and $\rho_{\perp s}$ are the longitudinal and transverse magnetoresistivities extrapolated to $H_{int}=H_{ext}-H_{demag}=0$, respectively; H_{ext} is the external magnetic field and H_{demag} is the demagnetizing field which depends on the dimensions of the sample and its orientation with respect to H_{ext}. Compared to the amount of data taken on the galvanomagnetic coefficients such as electrical resistivity and the Hall effect, relatively few data have been reported[1–6] on the SRA of amorphous TM-M alloys. Almost all the experimental efforts made so far have centered around an expression for the SRA in terms of the spontaneous magnetization of the type $\Delta\rho_s/\rho_0=A\bar{\mu}^n$, where $\bar{\mu}$ is the average saturation magnetic moment per TM atom, and A and n are constants. However, values of n ranging from 1–8 (Refs. 2 and 4–6) have been obtained from the data taken on different alloy systems at different temperatures, an observation which implies that such a relation between SRA and $\bar{\mu}$ is of little physical significance. No attempts have been made until now to ascertain which of the existing theories correctly describes the experimental results on SRA of amorphous ferromagnetic alloys.

With this aim in mind, a detailed investigation of SRA on amorphous $(Fe\text{-}Ni)_{80}B_{20}$ and $(Fe\text{-}Ni)_{80}P_{14}B_6$ alloy series was undertaken. The results of such a study are presented and discussed in terms of various theoretical models. It is shown that the split-band (SB) model, which could provide a satisfactory explanation for the observed composition dependence of linear saturation magnetostriction λ_s, spontaneous Hall effect R_s, and the coefficient of the electronic specific heat γ in these metallic glasses, fails to account for the present observations. By comparison, the two-current conduction (TCC) model provides not only a straightforward explanation for the variation of SRA with composition observed in the investigated alloy series but also conclusive evidence for a transition from weak to strong ferromagnetism at a concentration $x\simeq 60$ at. % in amorphous $Fe_xNi_{80-x}P_{14}B_6$ alloy series and for weak ferromagnetism in the $Fe_xNi_{80-x}B_{20}$ metallic glass system in the entire composition range. This

evidence is further supported by the high-field susceptibility data.

II. EXPERIMENTAL

Amorphous alloy ribbons having cross sections in the range $(1.0-2.2)\times(0.025-0.035)$ mm^2 were prepared by the single-roller quenching technique.[7] While it is possible to make all the compositions ($0<x<80$ at. %) in the $Fe_xNi_{80-x}P_{14}B_6$ alloy series in the amorphous state, the alloys with $x<20$ at. % in the $Fe_xNi_{80-x}B_{20}$ alloy series can be obtained in the amorphous form only when 1 at. % B is replaced by Si. Note that the nominal compositions x of these alloys used throughout this work are all in atomic percent.

A four-probe dc method was used to measure the electrical resistivity to a relative accuracy of better than 1 part in 10^5. However, the absolute accuracy of the resistivity measurements was as low as 4% because of the large uncertainty in the measurement of the ribbon thickness. The voltage contacts consisted of very thin Al wires bonded to the sample by the ultrasonic method. The magnetoresistivity of the amorphous ribbons was measured at 4.2 K in magnetic fields up to 3 and 7 kOe, respectively, applied parallel and perpendicular to the long axis of the ribbon (the current direction) in the ribbon plane. A current value of 100 mA, maintained constant to better than 1 part in 10^6, was passed through the sample during the measurement period. The temperature before and after the measurements was monitored by a precalibrated Ge thermometer in order to check the drift in temperature, if any. Magnetic measurements on the samples in question were performed at 4.2 K in fields up to 15 kOe using the Faraday method.

III. RESULTS AND DISCUSSION

The typical magnetoresistivity behavior of the investigated alloys is depicted in Fig. 1. In this figure the magnetoresistivity versus magnetic field plots for both longitudinal and transverse configurations are shown for a few chosen compositions in the amorphous $Fe_xNi_{80-x}B_{20}$ alloy system. It is noted that the longitudinal magnetoresistivity $\Delta\rho_{||}/\rho_0$ is positive while the transverse magnetoresistivity $\Delta\rho_{\perp}/\rho_0$ is negative, and both show a tendency towards saturation as the external magnetic field H_{ext} increases; the technical saturation in $\Delta\rho_{||}/\rho_0$ is achieved at a lower field value than that in $\Delta\rho_{\perp}/\rho_0$. The latter observation implies that the domain rotation processes occur at lower applied magnetic fields for the longitudinal geometry than that for the transverse one. Moreover, the magnetic fields at which the $\Delta\rho_{\perp}/\rho_0$ curves tend to saturate increase

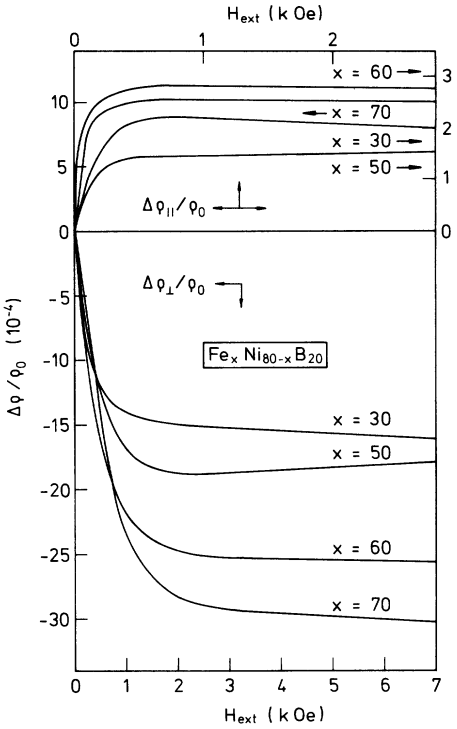

FIG. 1. Longitudinal $\Delta\rho_{||}/\rho_0$ and transverse $\Delta\rho_{\perp}/\rho_0$ magnetoresistivities at 4.2 K as a function of the external magnetic field H_{ext}, for a few chosen compositions in the amorphous alloy series $Fe_xNi_{80-x}B_{20}$.

with Fe concentration x while the $\Delta\rho_{||}/\rho_0$ curves do *not* exhibit any *systematic* trend (note that Fig. 1, which correctly represents the saturation behavior shown by the $\Delta\rho_{\perp}/\rho_0$ vs H_{ext} curves for all the alloys studied in this work, shows that $\Delta\rho_{||}/\rho_0$ tends to saturate at a field value which decreases with increasing x, a trend which is *not valid* for all the samples in a given alloy series). The above trend could result from the fact that the demagnetizing field $H_{demag}=4\pi NM$ (where N is the demagnetizing factor and M is the saturation magnetization at 4.2 K) increases with increasing x for the $\Delta\rho_{\perp}/\rho_0$ case since M increases with increasing x while N remains roughly constant, whereas in the $\Delta\rho_{||}/\rho_0$ case $H_{demag}\simeq 0$ and hence even a small variation in N leads to a change in H_{demag} which could be much larger than that caused by the increase in M with x. As mentioned above, $H_{demag}\simeq 0$ for the longitudinal case so that $H_{int}\simeq H_{ext}$. For the transverse configuration, H_{demag} was estimated from the dimensions of the samples and their corresponding values for the saturation magnetization at 4.2 K.[8] The values of the demagnetizing factor so obtained range from $(1.0-1.5)\times 10^{-2}$. The estimation of the quantity ρ_0 is not straightforward since the expression

$\rho_0=\frac{1}{3}\rho_{\|s}+\frac{2}{3}\rho_{\perp s}$ normally used in the literature[2–4] is not valid for the amorphous magnetic alloys owing to the fact that in these systems the assumption, made to obtain the above expression for ρ_0, that a perfectly random distribution in the orientation of spontaneous magnetization exists, no longer holds. For example, domain observations[9] on amorphous $Fe_{80}B_{20}$ (Metglas® 2605) have revealed that in this alloy the easy direction of magnetization lies at an angle of 60° with the ribbon axis lying in the plane of the ribbon. Additional support to the above argument is provided by the observation that for the present amorphous ferromagnets $|\Delta\rho_{\perp s}/\rho_0| \gg |\Delta\rho_{\|s}/\rho_0|$, where $\Delta\rho_{\|s}/\rho_0$ and $\Delta\rho_{\perp s}/\rho_0$ values are obtained by extrapolating the high-field portions of the $\Delta\rho_{\|}/\rho_0$ vs H_{ext} and $\Delta\rho_{\perp}/\rho_0$ vs H_{ext} curves to $H_{int}=0$ (i.e., $H_{int}\simeq H_{ext}=0$ for the longitudinal case and $H_{demag}=H_{ext}$ for the transverse case), while the relation[10] $|(\Delta\rho_{\|s}/\rho_0)/(\Delta\rho_{\perp s}/\rho_0)|=2$ is obtained in case all orientations of spontaneous magnetization are equally probable. We have taken ρ_0 to equal the resistivity value at 4.2 K in absence of the field for twofold reasons. First, the magnetoresistivity is quite small. Second, this choice will certainly introduce less error in the determination of SRA than that introduced by the uncertainty in the measurements of sample thickness.

All the alloys, with the exception of the composition $Fe_{50}Ni_{30}B_{20}$ (Fig. 1), exhibit a negative slope, i.e., the resistivity decreases at high fields, above technical saturation in both $\Delta\rho_{\|}/\rho_0$ and $\Delta\rho_{\perp}/\rho_0$. The negative slope values deduced directly from the plots similar to the ones shown in Fig. 1 by using the relations

$$[(1/\rho_0)(\partial\rho_{\|}/\partial H)]=\partial(\Delta\rho_{\|}/\rho_0)/\partial H$$

and

$$[(1/\rho_0)(\partial\rho_{\perp}/\partial H)]=\partial(\Delta\rho_{\perp}/\rho_0)/\partial H$$

are practically equal (to within 10%) for the longitudinal and transverse cases, and range from 0.5×10^{-8} Oe^{-1} to 2.5×10^{-8} Oe^{-1}, values that are in reasonable agreement with those previously reported[2,5] for some of the compositions in the present amorphous alloy series. The negative magnetoresistance observed after saturation can be explained in terms of both localized and band models. In the former model this effect is caused by the reduced electron-magnon scattering as the field increases, whereas in the latter model it is related to the slow increase of magnetization above saturation. The positive slope at high fields for the glassy $Fe_{50}Ni_{30}B_{20}$ is due to the positive contribution[10] to magnetoresistivity, arising from the Lorentz force acting on the conduction electrons, that completely masks the negative contribution to magnetoresistivity resulting from the ferromagnetism in this alloy. Although such a positive contribution to magnetoresistivity should be present for all the alloys in question, it is not clear as to why in this alloy only this contribution is so large as to completely overwhelm the negative ferromagnetic contribution. Since the high-field slopes for a given alloy are the same for $\Delta\rho_{\|}/\rho_0$ and $\Delta\rho_{\perp}/\rho_0$, it is expected that this positive contribution affects the slopes in $\Delta\rho_{\|}/\rho_0$ and $\Delta\rho_{\perp}/\rho_0$ to the same extent and hence will not cause any ambiguity in determining SRA. This is verified by the finding that SRA

$$\Delta\rho_s/\rho_0=(\Delta\rho_{\|s}/\rho_0)-(\Delta\rho_{\perp s}/\rho_0)$$

values presently determined for the amorphous $Fe_xNi_{80-x}B_{20}$ and $Fe_xNi_{80-x}P_{14}B_6$ alloys conform very well with the values at 0 K, obtained from a study[4] of $\Delta\rho_s/\rho_0$ at different temperatures, and with those measured[6] at 77 K for some of the present compositions (see Figs. 2 and 3). Thus the SRA values reported here represent the inherent property of the studied amorphous ferromagnetic alloys. The composition dependence of SRA is shown in Figs. 2 and 3. Note that in Fig. 2 the data obtained on the Ni-rich alloys, i.e., the alloys in the series $Fe_xNi_{80-x}B_{19}Si_1$ with $x=10$, 13, and 16, present a variation with x which joins smoothly with that observed for higher values of x in the alloy series $Fe_xNi_{80-x}B_{20}$. This observation is in conformity with the conclusion that SRA is not influenced by

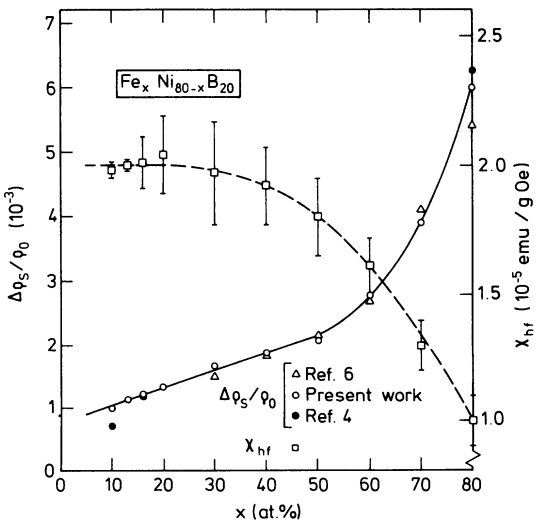

FIG. 2. Composition dependence of the spontaneous resistivity anisotropy $\Delta\rho_s/\rho_0$ and the high-field magnetic susceptibility χ_{hf} for $Fe_xNi_{80-x}B_{20}$ glasses. The results on $\Delta\rho_s/\rho_0$ taken at 0 K (closed circles) and 77 K (open triangles) are taken from Refs. 4 and 6, respectively.

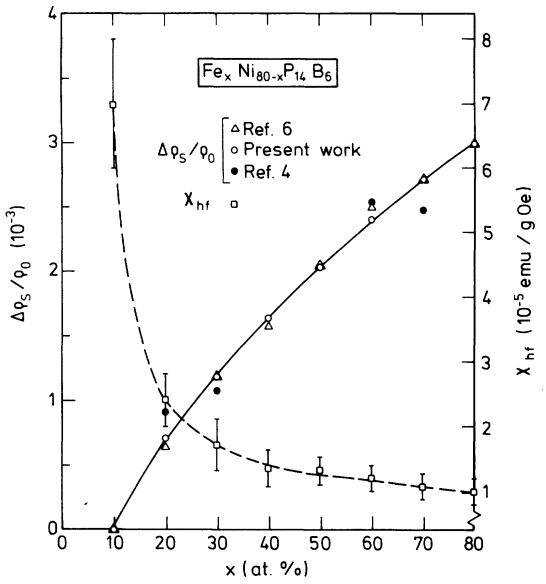

FIG. 3. $\Delta\rho_s/\rho_0$ and χ_{hf} as a function of the Fe concentration x in the amorphous $Fe_xNi_{80-x}P_{14}B_6$ alloys. $\Delta\rho_s/\rho_0$ values at 0 K (closed circles) and 77 K (open triangles) included in this figure are taken from Refs. 4 and 6, respectively.

replacing B by Si recently drawn by Yao *et al.*[6] from the study of SRA in amorphous $Fe_{80}B_{20}$ and $Fe_{80}B_{14}Si_6$ alloys. In the following text the results shown in Figs. 2 and 3 are discussed in the light of SB and TCC models.

A. SB model

In crystalline Ni-Fe alloys, SRA goes through a maximum whereas the linear saturation magnetostriction λ_s and the spontaneous Hall coefficient R_s both go to zero and change sign at approximately the same electron concentration,[11] 27.70 ± 0.05 e/atom (or $C_{Fe}\simeq0.18$, where C_{Fe} is the atomic concentration of Fe). Based on the SB model, which describes the spin-down $3d$ ($3d_\downarrow$) band of the binary Ni-Fe alloy as shown in Fig. 4 [i.e., Ni and Fe have their own $3d_\downarrow$ bands distinct from each other on the energy scale and that the spin-up $3d$ ($3d_\uparrow$) band can be ignored since it is full], Berger[11–14] has shown that the above-mentioned anomalies in various properties of Ni-Fe alloys occur at the alloy composition at which the Fermi level E_F is located at the boundary (the point T in Fig. 4) between Ni $3d_\downarrow$ and Fe $3d_\downarrow$ bands. At this critical composition, the number of $3d$ holes in the alloy should equal the number of states in the Fe $3d_\downarrow$ band, i.e.,

$$5C_{Fe}=2.55C_{Fe}+0.55C_{Ni}\ , \qquad (1)$$

with $C_{Fe}+C_{Ni}=1$. Equation (1) is satisfied when

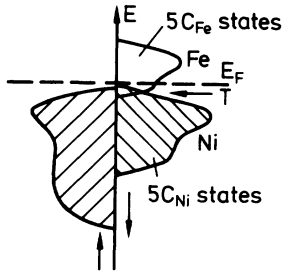

FIG. 4. SB model for the spin-down band of fcc Ni-Fe alloys.

$C_{Fe}=0.18$, in excellent agreement with the experimental observations.[11] A variety of experimental data on crystalline binary Fe–X (X=Cr,Mo, V,W,Ti,Nb) (Ref. 13) and ternary Ni-Fe-M (M=Cr,Mo,V,Cu,W) (Refs. 12 and 14) alloys, and the detailed coherent potential approximation calculations[15] on Ni-Fe alloys support the validity of this model. Recently, the SB model has been applied by O'Handley *et al.*[16,17] to describe the composition variations of the $R_s=\lambda_s=0$ lines in amorphous (Fe-Co-Ni)$_{80}$B$_{20}$ alloys (the agreement between the experimentally observed and theoretically predicted variation was found to be very good particularly for the glasses on the Fe-Ni-rich side, where due to the larger nuclear charge difference the SB model is more applicable), and by Onn[18] to provide a qualitative explanation for the experimental variation of the electronic specific-heat coefficient γ with Fe concentration in amorphous (Fe-Ni)$_{80}$B$_{20}$ and (Fe-Ni)$_{80}$P$_{14}$B$_6$ alloys.

For the (Fe-Ni)$_{80}$B$_{20}$ and (Fe-Ni)$_{80}$P$_{14}$B$_6$ glasses, Eq. (1) can be generalized to[17]

$$5C_{Fe}=2.55C_{Fe}+0.55C_{Ni}-1.6C_B\ , \qquad (2)$$

with $C_{Fe}+C_{Ni}=0.8$, $C_B=0.2$ and

$$5C_{Fe}=2.55C_{Fe}+0.55C_{Ni}-2.4C_P-1.6C_B\ , \qquad (3)$$

with $C_{Fe}+C_{Ni}=0.8$, $C_P=0.14$, $C_B=0.06$, respectively. The glass formers boron and phosphorus have been found to contribute an average of 1.6 electrons per B atom and 2.4 electrons per P atom to the TM $3d$ bands.[19] Equations (2) and (3) predict $C_{Fe}\simeq0.04$ and 0.003 for $R_s=\lambda_s=0$, and the maximum in SRA in amorphous (Fe-Ni)$_{80}$B$_{20}$ and (Fe-Ni)$_{80}$P$_{14}$B$_6$ alloys, respectively. While λ_s appears to go to zero near this concentration in the former alloy series, the highest value of SRA is reached in both the alloy systems at $C_{Fe}=0.8$, a result which directly contradicts[20] the prediction of the SB model. Thus the SB model fails to account for the composition dependence of SRA in the metallic glasses studied in this work.

B. TCC model

Present results are now discussed within the framework of the TCC model, which has had tremendous success in explaining a large amount of experimental data on the transport properties of crystalline Fe- and Ni-based alloys.[21–25] In this model, spin-up and spin-down electrons conduct in parallel and the SRA is a consequence of the anisotropic $d_\uparrow$-$d_\downarrow$ mixing caused by the spin-orbit interaction.[26] Calculations based on this model yield the following expressions for SRA at low temperatures[25]:

$$\frac{\Delta\rho_s}{\rho_0}=\gamma(\alpha-1)+3\beta\frac{\alpha}{(\alpha+1)}\ , \tag{4a}$$

where

$$\alpha=\frac{\rho_\downarrow^0}{\rho_\uparrow^0}\ , \tag{4b}$$

$$\beta=-\frac{7}{90}\left[\frac{\lambda'}{\Delta}\right]^2(1-4\cos^2\eta_2^\uparrow)\sin^2\eta_2^\uparrow\ , \tag{4c}$$

$$\gamma=\frac{3}{4}\left[\frac{\lambda}{H_{\rm ex}}\right]^2\ , \tag{4d}$$

$\rho_\uparrow^0$ and $\rho_\downarrow^0$ are the residual resistivities for spin-up and spin-down electrons, respectively, λ' is the *local* spin-orbit coupling constant, Δ is the virtual bound state width, $\eta_2^\uparrow$ is the phase shift, λ is the average value of the spin-orbit coupling constant in the d band, and $H_{\rm ex}$ is the exchange energy that splits the $d_\uparrow$ and $d_\downarrow$ bands. For the first transition-metal series, $\lambda'\ll\Delta$ and hence the second term in Eq. (4a) can be safely neglected for the present alloys. Furthermore, γ has been estimated to be $\simeq$0.01 (Ref. 25) from a large amount of experimental data on the SRA of Fe- and Ni-based alloys. With the neglect of the second term, Eq. (4a) becomes

$$\frac{\Delta\rho_s}{\rho_0}=\gamma(\alpha-1)\ . \tag{5}$$

Equation (5) provides a criterion for determining whether a given alloy is a "strong" or a "weak" ferromagnet (a strong ferromagnet has holes only in the $d_\downarrow$ band while a weak ferromagnet has holes and electrons in both $d_\uparrow$ and $d_\downarrow$ bands) as follows: $\rho_\downarrow^0$ and $\rho_\uparrow^0$ possess comparable values for a weak ferromagnet since vacant states are available in both $d_\uparrow$ and $d_\downarrow$ for s electrons to make transitions, whereas the value of $\rho_\downarrow^0$ greatly exceeds that of $\rho_\uparrow^0$ in a strong ferromagnet because s-d scattering is allowed only for spin-down electrons as there are no vacant $d_\uparrow$ states at the Fermi level. Thus according to Eq. (5), $\Delta\rho_s/\rho_0$ is expected to be very large for strong ferromagnets and small for weak ferromagnets. In this context the alloys on the Ni-rich side (Fe-rich side) in both amorphous $Fe_xNi_{80-x}B_{20}$ and $Fe_xNi_{80-x}P_{14}B_6$ alloy systems are expected to be weak (strong) ferromagnets. The high-field susceptibility $\chi_{\rm hf}$ measurements (whose results are also included in Figs. 2 and 3) taken at 4.2 K also support this viewpoint when one realizes that within the band picture $\chi_{\rm hf}$ should possess very large values for weak ferromagnets and small values for strong ferromagnets. Though the present $\chi_{\rm hf}$ measurements have been carried out in fields up to only 15 kOe, the $\chi_{\rm hf}$ values obtained for $Fe_{80}B_{20}$ and $Fe_{80}P_{14}B_6$ alloys are in excellent agreement with those determined for these alloys from very high-field (100–300 kOe) susceptibility measurements.[27,28] The unusually large value of $\chi_{\rm hf}$ for glassy $Fe_{10}Ni_{70}P_{14}B_6$ is a manifestation of the fact that this alloy exhibits spin-glass behavior[29] at low temperatures. In the band model, the above variation of $\chi_{\rm hf}$ with x is expected to get reflected in the magnitude of the negative slopes at high fields, i.e., a large negative high-field slope for weak ferromagnets and a small negative slope value for strong ferromagnets. We do not observe the expected trend in the high-field slope values for our alloys presumably due to the fact that actual variation is made obscure by the significant positive contribution to magnetoresistivity arising from the Lorentz force, as already mentioned. It is shown in the following text that the above classification of weak and strong ferromagnets is not so conclusive as it would seem to be at first sight.

With a view to derive some information about the electronic structure of the investigated alloys, we now proceed to compute $\rho_\downarrow^0(x)$ and $\rho_\uparrow^0(x)$ from the relations

$$\rho_\downarrow^0(x)=\rho^0(x)\left[\gamma^{-1}\left[\frac{\Delta\rho_s}{\rho_0}(x)\right]+2\right] \tag{6}$$

and

$$\rho_\uparrow^0(x)=\rho_\downarrow^0(x)\left[\gamma^{-1}\left[\frac{\Delta\rho_s}{\rho_0}(x)\right]+1\right]^{-1}\ , \tag{7}$$

obtained by combining Eq. (5) with the expression given by the TCC model for the residual resistivity ρ^0, i.e.,

$$\rho^0=\frac{\rho_\uparrow^0\rho_\downarrow^0}{(\rho_\uparrow^0+\rho_\downarrow^0)}=\frac{\rho_\downarrow^0}{(1+\alpha)}\ . \tag{8}$$

We do not distinguish between the values of resistivity at 0 K (ρ^0) and those of 4.2 K (ρ_0) because the difference between the two sets of values, if any, is expected to fall within the error limits of the resistivity measurements. The $\rho_\downarrow^0$, $\rho_\uparrow^0$ and α (equal to

$\rho_{\downarrow}^0/\rho_{\uparrow}^0$) values for different alloy compositions computed using Eqs. (6) and (7) while taking $\rho^0=\rho_0=\rho(4.2\ \text{K})$ are shown in Figs. 5 and 6. It is noted from these figures that for $Fe_xNi_{80-x}B_{20}$ glasses, both $\rho_{\uparrow}^0$ and $\rho_{\downarrow}^0$ as a function of x increase at a fixed rate up to $x\simeq 50$, beyond which $\rho_{\downarrow}^0$ increases at a rate that is much steeper than that for $x<50$ and $\rho_{\uparrow}^0$ decreases, whereas for $Fe_xNi_{80-x}P_{14}B_6$ amorphous alloys, $\rho_{\downarrow}^0$ increases roughly at a constant rate while $\rho_{\uparrow}^0$ decreases till a value $x\simeq 60$ is reached beyond which the rate of increase in $\rho_{\downarrow}^0$ progressively slows down and $\rho_{\uparrow}^0$ remains practically constant. By remembering that the residual resistivity is directly proportional to the density of states at the Fermi level $N(E_F)$, which, in turn, varies with composition, the composition dependence of $\rho_{\uparrow}^0$ and $\rho_{\downarrow}^0$ shown in Figs. 5 and 6 can be interpreted as follows: In glassy $Fe_xNi_{80-x}B_{20}$ alloys the probability for s electrons to get scattered to the $d_{\uparrow}$ and $d_{\downarrow}$ bands is almost equal (the $s_{\downarrow}$-$d_{\downarrow}$ transitions becoming more and more frequent than the $s_{\uparrow}$-$d_{\uparrow}$ transitions as x increases) for low values of x since $N(E_F)$ possesses comparable values for the $d_{\uparrow}$ and $d_{\downarrow}$ bands. This situation continues till $x\simeq 50$ beyond which $s_{\downarrow}$-$d_{\downarrow}$ scattering increases at the expense of $s_{\uparrow}$-$d_{\uparrow}$ scattering because $N(E_F)$ goes on increasing for the $d_{\downarrow}$ band while it progressively decreases for the $d_{\uparrow}$ band. At $x=80$, holes exist in both $d_{\uparrow}$ and $d_{\downarrow}$ bands, the number of holes in the latter band being much larger than that in the former band. This implies that $Fe_{80}B_{20}$ represents an alloy composition which is on the verge of becoming a strong ferromagnet, and if either the boron content is increased at the cost of Fe or a part of the boron content is replaced by phosphorus as in $Fe_{80}P_{14}B_6$, a transition to strong ferromagnetism is expected[30] when the excess transferred charge fills up all the

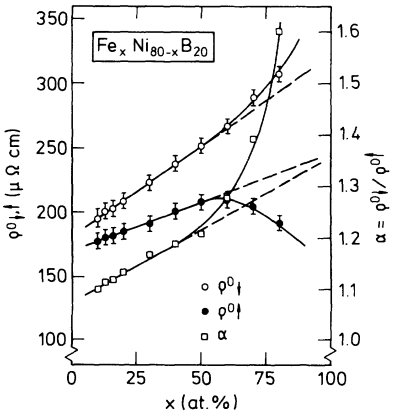

FIG. 5. Dependence of the spin-up $\rho_{\uparrow}^0$ and spin-down $\rho_{\downarrow}^0$ residual resistivities of their ratio α on the Fe concentration x in amorphous $Fe_xNi_{80-x}B_{20}$ alloy series.

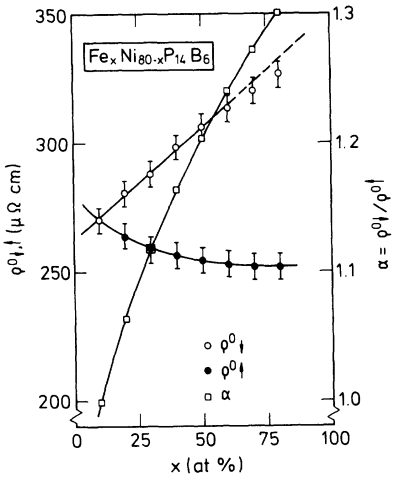

FIG. 6. $\rho_{\downarrow}^0$, $\rho_{\uparrow}^0$, and their ratio α (equal to $\rho_{\downarrow}^0/\rho_{\uparrow}^0$) as a function of Fe concentration x in the amorphous $Fe_xNi_{80-x}P_{14}B_6$ alloy series.

holes in the $d_{\uparrow}$ band. In the case of amorphous $Fe_xNi_{80-x}P_{14}B_6$ alloys, on the other hand, the probability for $s_{\downarrow}$-$d_{\downarrow}$ transitions increases while for $s_{\uparrow}$-$d_{\uparrow}$ transitions it decreases, since $N(E_F)$ increases for the $d_{\downarrow}$ band while it decreases for the $d_{\uparrow}$ band as the Fe concentration x is increased from the low-x limit, till at $x\simeq 60$ a transition to strong ferromagnetism occurs. Beyond $x=60$, $\rho_{\uparrow}^0$ remains constant, whereas $\rho_{\downarrow}^0$ continues to increase because the spin-up electrons now get scattered only to the broad $s_{\uparrow}$ band [the role of s band for the spin-up electrons, in particular, now or even below $x\simeq 60$, becomes very important and hence can no longer be ignored, and because the s band is very broad, $N(E_F)$ for spin-up electrons remains practically constant] as there are no vacant states available in the $d^{\uparrow}$ band, as contrasted with spin-down electrons which get scattering to both $s_{\downarrow}$ and $d_{\downarrow}$ bands [the $s_{\downarrow}$-$d_{\downarrow}$ scattering still dominates over $s_{\downarrow}$-$s_{\downarrow}$ scattering since $N_{d_{\downarrow}}(E_F)\gg N_{s_{\downarrow}}(E_F)$]. Therefore the alloys with compositions in the range $60<x<80$ in this alloy series are strong ferromagnets while those having $x<60$ are weak ferromagnets. The above classification of weak and strong ferromagnets in the investigated glassy alloy series is consistent[31] with the variation of magnetic moment with composition in these alloys.

Figures 2 and 3 also present another interesting feature that when B in the amorphous $Fe_xNi_{80-x}B_{20}$ alloy system is partly replaced by P, as in glassy $Fe_xNi_{80-x}P_{14}B_6$ alloys, the SRA values are *not significantly altered* in the concentration range $30<x<60$, but they are greatly *reduced* for alloys with $x>60$ (the reduction in SRA being the largest for the alloy with $x=80$) and for those with $x<30$

[Fig. 7(b)]. A similar trend with composition is shown by the electronic specific-heat coefficient $\gamma=(\pi^2k_B^2/3)N(E_F)$ data [see Fig. 7(a)] previously taken on the same alloy series as ours by Onn and his co-workers.[32] By realizing that P donates roughly twice[19] as many electrons per atom to the TM d bands as B does, the excess charge transferred from the metalloid atoms is shared by both $d_\uparrow$ and $d_\downarrow$ bands for x in the range $30<x<60$, a result which not only affects $\rho_\uparrow^0$ and $\rho_\downarrow^0$ roughly to the same extent and hence leaves SRA practically unaltered [Eq. (5)] but also has little or even no effect on $N(E_F)$ [Fig. 7(a)]. For $x>60$, the excess transferred charge is totally effective in filling up the holes in the $d_\downarrow$ band since there are no holes left in the $d_\uparrow$ band, and as such both $N(E_F)$ and $\rho_\downarrow^0$ decrease very rapidly while hardly affecting $\rho_\uparrow^0$; a process which results in a rapid decrease of SRA for these compositions. By recalling that the magnetic moment exhibits a steep decrease particularly for the alloys with $x<30$ in the amorphous alloy series $Fe_xNi_{80-x}B_{20}$ (i.e., on the Ni-rich side),[8] the holes in both $d_\uparrow$ and $d_\downarrow$ bands are expected to become smaller and smaller in number and as a result the excess transferred charge should become more and more effective in filling up the $d_\uparrow$ and $d_\downarrow$ holes as x is lowered below $x=30$. Consequently, both $\rho_\downarrow^0$ $[N_{d_\downarrow}(E_F)]$ and $\rho_\uparrow^0$ $[N_{d_\uparrow}(E_F)]$ decrease at a very fast rate and their ratio $\alpha\rightarrow1$ as $x\rightarrow0$. This, in turn, leads to a significant reduction in both SRA and $N(E_F)$ in this concentration range. The above arguments not only lend a firm support to our earlier conclusions regarding the electronic structure of these alloys but also strongly suggest that a charge transfer takes place from the metalloid atoms to the TM d bands. A number of other experimental evidences, which also favor the charge-transfer mechanism invoked in this work, have been reported[31] in the past.

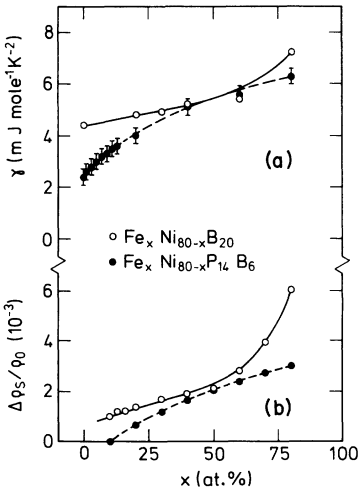

FIG. 7. Electronic specific-heat coefficient γ (a) and the spontaneous resistivity anisotropy $\Delta\rho_s/\rho_0$ (b) as a function of x in amorphous $Fe_xNi_{80-x}B_{20}$ and $Fe_xNi_{80-x}P_{14}B_6$ alloys. The data shown in (a) are taken from Ref. 32.

Finally, we focus our attention on the relation between SRA and the saturation magnetic moment per transition-metal atom at 0 K, $\bar{\mu}$, of the type $\Delta\rho_s/\rho_0=A\bar{\mu}^n$. The values of $\bar{\mu}$ for the present alloys have been taken from our previous investigation.[8] Figure 8 shows the $\ln[(\Delta\rho_s/\rho_0)\times10^3]$ vs $\ln\bar{\mu}$ plots. It is noted that such a plot is a straight line for the amorphous $Fe_xNi_{80-x}P_{14}B_6$ alloy system with the values $A=(1.3\pm0.1)\times10^{-3}$ and $n=1.4\pm0.1$. For the $Fe_xNi_{80-x}B_{20}$ glasses, the data can be fitted to two straight lines; one for compositions below $x=50$ and the other for the alloys with $x\geq60$ with the choice of parameters as $A=(1.6\pm0.1)\times10^{-3}$ and $n=0.62\pm0.02$, and $A=(1.6\pm0.1)\times10^{-4}$ and $n=5.0\pm0.1$, respectively. This observation implies that SRA and $\bar{\mu}$ are not so simply related to each other as the expression $\Delta\rho_s/\rho_0=A\bar{\mu}^n$ would suggest. Efforts to directly relate SRA with $\bar{\mu}$ have failed[24] even in the case of crystalline ferromagnetic alloys.

IV. CONCLUSIONS

The results of the present magnetoresistivity and high-field susceptibility measurements permit us to draw the following conclusions:

(i) The SB model fails to predict the correct trend for spontaneous resistivity anisotropy in the investigated glassy alloy series.

(ii) By contrast, the TCC model provides not only a straightforward explanation for the observed re-

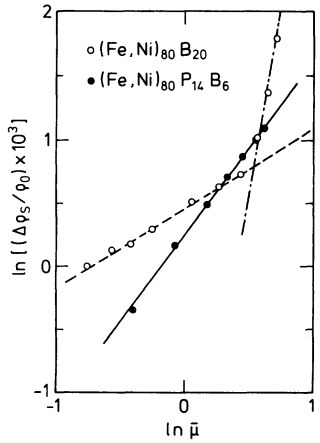

FIG. 8. $\ln[(\Delta\rho_s/\rho_0)\times10^3]$ vs $\ln\bar{\mu}$ at 4.2 K for the present amorphous alloy series.

sults but also a conclusive evidence for a transition from weak to strong ferromagnetism at a concentration $x \simeq 60$ in amorphous $Fe_xNi_{80-x}P_{14}B_6$ alloy series and for weak ferromagnetism in glassy $Fe_xNi_{80-x}B_{20}$ alloys in the entire concentration range. This evidence for weak and strong ferromagnetism in these glasses is further supported by the high-field susceptibility data.

(iii) A charge transfer takes place from the metalloid atoms to the transition-metal d bands.

(iv) Spontaneous resistivity anisotropy cannot be related to the saturation magnetic moment per transition-metal atom by so simple a relation as $\Delta\rho_s/\rho_0 = A\bar{\mu}^n$.

ACKNOWLEDGMENTS

The finanical assistance provided by the Deutsche Forschungsgemeinschaft to carry out this work is gratefully acknowledged.

[1]Y. Obi, H. Fujimori, and H. Morita, Sci. Rep. Res. Inst. Tohoku Univ. Ser. 1 26, 214 (1977); Z. Marohnic, E. Babic, and D. Pavna, Phys. Lett. 63A, 348 (1977).

[2]G. Böhnke, N. Croitoru, M. Rosenberg, and M. Sostarich, IEEE Trans. Magn. 14, 955 (1978); A. K. Nigam and A. K. Majumdar, Physica 95B, 385 (1978).

[3]R. Kern and U. Gonser, J. Magn. Magn. Mater. 13, 74 (1979); 21, 182 (1980).

[4]G. Böhnke and M. Rosenberg, J. Phys. (Paris) Colloq. 41, C8-481 (1980).

[5]M. Naka, R. Kern, and U. Gonser, J. Appl. Phys. 52, 1448 (1981); J. Yamasaki, H. Fukunaga, and K. Narita, *ibid.* 52, 2202 (1981).

[6]Y. D. Yao, S. Arajs, and S. T. Lin, J. Appl. Phys. 53, 2258 (1982).

[7]H. H. Lieberman and C. D. Graham, Jr., IEEE Trans. Magn. 12, 921 (1976).

[8]S. N. Kaul, IEEE Trans. Magn. 17, 1208 (1981).

[9]R. Hasegawa, R. C. O'Handley, and L. I. Mendelsohn, in *Magnetism and Magnetic Materials—1976 (Joint MMM-Intermag Conference, Pittsburgh),* Partial Proceedings of the First Joint MMM-Intermag Conference, edited by J. J. Becker and G. H. Lander (AIP, New York, 1977), p. 298.

[10]J.-P. Jan, in *Solid State Physics,* edited by F. Seitz and D. Turnbull, (Academic, New York, 1957), Vol. 5, p. 1.

[11]L. Berger, Physica 30, 1141 (1964); Phys. Rev. 138, A1083 (1965).

[12]H. Ashworth, D. Sengupta, G. Schnakenberg, L. Shapiro, and L. Berger, Phys. Rev. 185, 782 (1969).

[13]L. Berger, in *Magnetism and Magnetic Materials—1976 (Joint MMM-Intermag Conference, Pittsburgh),* Partial Proceedings of the First Joint MMM-Intermag Conference, edited by J. J. Becker and G. H. Lander (AIP, New York, 1977), p. 355.

[14]L. Berger, Physica 91B, 31 (1977).

[15]H. Hasegawa and J. Kanamori, J. Phys. Soc. Jpn. 31, 382 (1971); 33, 1599 (1972).

[16]R. C. O'Handley and L. Berger, in *Proceedings of the International Conference on the Physics of Transition Metals, Toronto, 1977,* edited by M. J. G. Lee, J. M. Perz, and E. Fawcett (IOP, London, 1978), p. 477.

[17]R. C. O'Handley, Phys. Rev. B 18, 930 (1978); 18, 2577 (1978).

[18]D. G. Onn, J. Appl. Phys. 52, 1788 (1981).

[19]R. C. O'Handley, R. Hasegawa, R. Ray, and C.-P. Chou, Appl. Phys. Lett. 29, 330 (1976); J. Appl. Phys. 48, 2095 (1977).

[20]Different values for the electrons per atom that boron and phosphorus atoms donate to the TM bands have been reported (see, e.g., Refs. 8 and 27). Even with these values, the maximum in SRA in the SB model is expected to occur on the Ni-rich side and *not* on the Fe-rich side where SRA is found to attain very large values.

[21]I. A. Campbell, A. Fert, and O. Jaoul, J. Phys. C 3, S95 (1970).

[22]M. C. Cadeville and B. Loegel, J. Phys. F 3, L115 (1973).

[23]I. A. Campbell, J. Phys. F 4, L181 (1974); A. Fert and I. A. Campbell, *ibid.* 6, 849 (1976).

[24]S. N. Kaul, J. Phys. F 7, 2091 (1977).

[25]O. Jaoul, I. A. Campbell, and A. Fert, J. Magn. Magn. Mater. 5, 23 (1977).

[26]J. Smit, Physica (Utrecht) 16, 612 (1951).

[27]K. Fukamichi, M. Kikuchi, H. Hiroyoshi, and T. Masumoto, in *Proceedings of the Third International Conference on Rapidly Quenched Metals.,* edited by B. Cantor (The Metals Society, London, 1978), p. 117.

[28]C. J. Beers, H. W. Myron, C. J. Schinkel, and I. Vincze, Solid State Commun. 41, 631 (1982).

[29]S. N. Kaul, Solid State Commun. 36, 279 (1980).

[30]S. N. Kaul, Phys. Status Solidi (in press).

[31]R. C. O'Handley and D. S. Boudreaux, Phys. Status Solidi A 45, 607 (1978).

[32]T. A. Donnelly, T. Egami, and D. G. Onn, Phys. Rev. B 20, 1211 (1979); J. K. Krause, T. C. Long, T. Egami, and D. G. Onn, *ibid.* 21, 2886 (1980); D. G. Onn, A. Sundermier, and J. K. Krause, J. Appl. Phys. 52, 1802 (1981).